

Fracture-resistance testing of pipeline girth welds using bend and tensile fracture specimens

by Prof. Claudio Ruggieri* and Leonardo L S Mathias

Department of Naval Architecture and Ocean Engineering, University of São Paulo, São Paulo, Brazil

STRUCTURAL-INTEGRITY ASSESSMENTS of pipe girth welds play a key role in the design and safe operation of pipeline systems. Current practices for structural-integrity assessments advocate the use of geometry-dependent resistance curves so that crack-tip constraint in both the test specimen and the structural component is similar. Thus, testing standards now under development to measure fracture resistance of pipeline steels often employ single-edge-notched (SE(T)) specimens under tension. This paper presents an investigation of the ductile-tearing properties for a girth weld of an API 5L X-80 pipeline steel using experimentally measured crack-growth-resistance curves (also termed *J-R* curves). Testing of the girth-weld pipeline steels employed clamped SE(T) specimens and three-point bend (SE(B)) specimens with weld centreline cracks to determine the *J*-resistance curves. The experimental toughness data enables further evaluation of crack growth resistance properties of pipeline girth welds.

THE ENGINEERING APPLICATION of fracture mechanics remains invaluable in assessments of macroscopic fracture behaviour and defect-analyses procedures of safety-critical structural components, including pressure vessels and pipeline girth welds. Fitness-for-service (FFS) fracture-assessment approaches, also referred to as engineering-critical assessment (ECA) procedures, rely upon a single parameter to define the crack-driving force and to characterize fracture resistance of the material [1-3]. These approaches provide a means for introducing acceptance criteria in cracked structural components by relating the operating conditions to a critical applied load or critical crack size. While a one-parameter description of applied loading in terms of the *J*-integral or the crack-tip-opening displacement (CTOD) and their corresponding macroscopic measures of fracture toughness (J_c or δ_c) [3] usually suffices to characterize the essentially stress-controlled failure by cleavage mode, quantitative analyses of fracture preceded and accompanied by extensive plastic deformation becomes more complex.

Low-constraint and structural components containing defects and flaws, including circumferentially cracked pipelines and their weldments made of high-grade,

high-toughness steels, often undergo significant stable crack growth (a) prior to material failure. Under sustained ductile tearing of a macroscopic crack, large increases in the load-carrying capacity for the flawed structural component are possible beyond the limits given by the onset of crack-growth initiation. Simplified engineering approaches for defect assessments, such as BS7910 [4] and API579 [5] methodologies, among others, incorporate the effects of ductile tearing on crack-driving forces to evaluate the severity of crack-like flaws in structural components in terms of crack-growth resistance ($J-a$) curves (also often denoted *J-R* curves) in which the *J*-integral fracture parameter characterizes the significant increase in toughness over the first few millimetres of stable crack extension (Da) [1,3].

Standardized techniques for crack-growth resistance testing of structural steels, including ASTM 1820 [6], routinely employ three-point bend (SE(B)) and compact-tension (C(T)) specimens containing deep, through cracks ($a/W \geq 0.45-0.50$). However, a variety of crack-like defects are most often surface cracks formed during in-service operation and exposure to aggressive environment or during welding fabrication. Structural components falling into this category include girth welds made in field conditions for high-pressure piping systems and steel catenary risers (SCRs). These crack configurations generally develop low levels of crack-tip stress triaxiality which contrast sharply to

*Corresponding author's contact details:
tel: +55 11 3091 5184
email: claudio.ruggieri@poli.usp.br

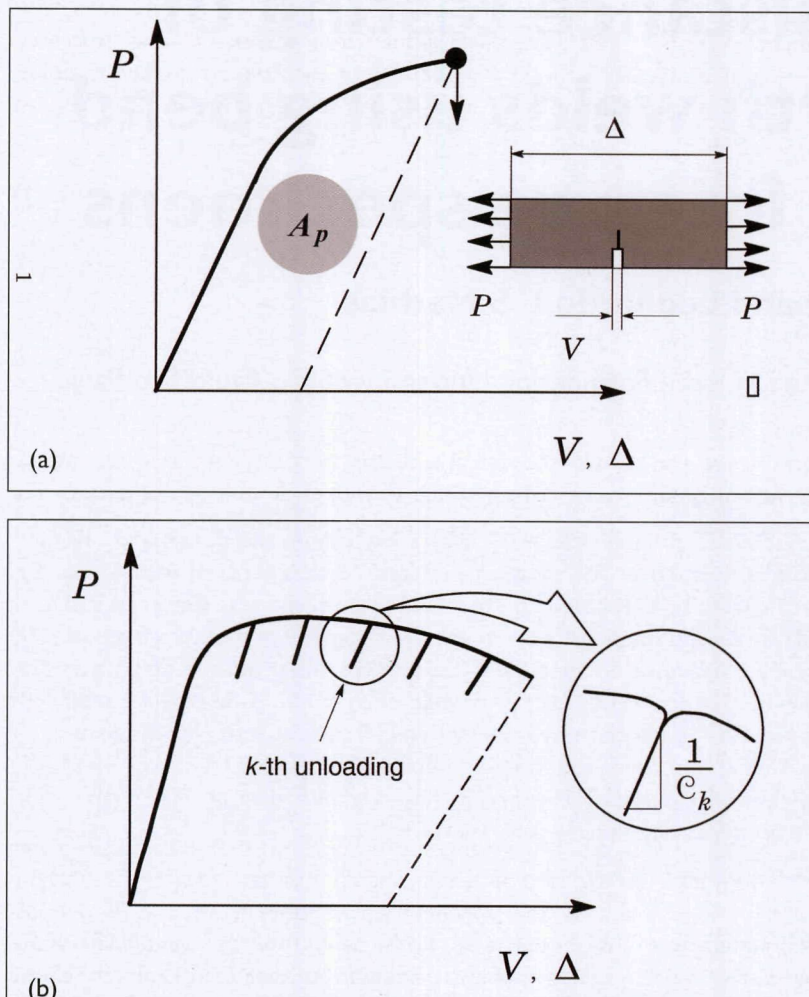


Fig. 1. (a) Partial unloading during the evolution of load with displacement; (b) definition of the plastic area under the load-displacement curve.

conditions present in deeply cracked specimens [7]. Recent defect-assessment procedures advocate the use of geometry-dependent fracture-toughness values so that crack-tip constraint in both test specimen and structural component is similar. In particular, fracture-toughness values measured using single-edge-notch tension (SE(T)) specimens appear more applicable for characterizing the fracture resistance of pressurized pipelines and cylindrical vessels than standard, deep-notch, fracture specimens under predominantly bend loading [8-10].

Recent applications of SE(T) fracture specimens to characterize crack-growth-resistance properties in pipeline steels [11] have been effective in providing larger flaw tolerances while, at the same time, reducing the otherwise excessive conservatism which arises when measuring the material's fracture toughness based on high constraint, deeply-cracked SE(B) or C(T) specimens. However, some difficulties associated with SE(T) testing procedures raise concerns about the significance and qualification of measured crack-growth-resistance curves. While slightly more conservative, testing of shallow-crack-bend specimen configurations may become more attractive due to its simpler testing protocol and laboratory procedures, and the much smaller loads required to propagate the

crack. Although deeply-cracked SE(B) specimens are the preferred crack geometry often adopted in conventional defect-assessment methods, recent revisions of ASTM 1820 [6] and ISO 15653 [12] have also included J -estimation equations applicable to shallow-crack-bend specimens. Consequently, use of smaller specimens which yet guarantee adequate levels of crack-tip constraint to measure the material's fracture toughness becomes an attractive alternative.

This work presents an experimental investigation of the ductile-tearing properties for a girth weld made of an API 5L X-80 pipeline steel in terms of crack-growth-resistance curves. Use of these materials is motivated by the increasing demand in the number of applications for manufacturing high-strength pipes for the oil and gas industry. Testing of the pipeline girth welds employed side-grooved, clamped SE(T) specimens and three-point-bend SE(B) specimens with a weld-centreline notch and varying crack sizes to determine the crack-growth-resistance curves using the unloading compliance (UC) method and a single specimen technique. Recently developed compliance functions and η -factors applicable for SE(T) and SE(B) fracture specimens are introduced

to determine crack-growth-resistance curves from laboratory measurements of load-displacement records. Overall, these experimental results provide toughness data which enable further evaluation of crack-growth-resistance properties of pipeline girth welds.

Experimental evaluation of J -resistance curves

Conventional testing programmes to measure crack-growth resistance ($J\Delta a$) curves in metallic materials routinely employ the UC method based on a single specimen test. The estimation procedure used in ASTM E1820 standard [6] predominantly employs load-line displacement (LLD) records to measure fracture-toughness-resistance data incorporating a crack-growth correction for the J -integral. An alternative method which potentially simplifies the test procedure involves the use of crack-mouth-opening displacement (CMOD) to determine both the J -integral and the amount of crack growth. This section provides a brief overview of the analytical framework needed to evaluate data for common fracture specimens from laboratory measurements of load-displacement records. Attention is directed to an incremental procedure to obtain estimates of J and crack length for the SE(T) and SE(B) configurations based on CMOD data.

Incremental estimation procedure of the J -integral

The procedure to estimate crack-growth-resistance data considers the elastic and plastic contributions to the strain energy for a cracked body under Mode I deformation [3] so that the J -integral conveniently derives from its elastic component, J_e , and plastic term, J_p , as $J = J_e + J_p$. Here, an estimation scheme for the plastic component employs a plastic η -factor introduced by Sumpter and Turner [13] to relate the crack-driving force to the plastic area under the load versus LLD (or CMOD) for cracked configurations (see also Refs [14-16]) as illustrated in Fig.1(a). The procedure to estimate J_p based on the η -methodology has proven highly effective in testing protocols to measure fracture toughness in stationary cracks while, at the same time, retaining strong contact with the deformation plasticity definition of J .

However, the area under the actual load-displacement curve for a growing crack differs significantly from the corresponding area for a stationary crack (upon which the deformation definition of J is based) [3]. Consequently, the measured load-displacement records must be corrected for crack extension to obtain an accurate estimate of J -values with increased crack growth. A widely used approach (which forms the basis of current

standards such as ASTM E1820 [6]) to evaluate J with crack extension follows from an incremental procedure which updates J_e and J_p at each partial unloading point, denoted k , during the measurement of the load vs displacement curve depicted in Fig.1(b) as:

$$J^k = J_e^k + J_p^k \quad (1)$$

where the current elastic term is simply given by:

$$J_e^k = \left(\frac{K_l^2}{E'} \right)_k \quad (2)$$

and the current plastic term follows an incremental formulation which is applicable to CMOD data in the form [14-16] in Eqn 3 below, in which the geometry factor γ_{LLD} is evaluated from:

$$\gamma_{LLD}^{k-1} = \left[-1 + \eta_{J-LLD}^{k-1} - \left(\frac{b_{k-1}}{W\eta_{J-LLD}^{k-1}} \frac{d\eta_{J-LLD}^{k-1}}{d(a/W)} \right) \right] \quad (4)$$

In the above expressions, K_l is the elastic stress intensity factor for the cracked configuration, A_p represents the plastic area under the load-displacement curve, B_N is the net specimen thickness at the side groove roots ($B_N = B$ if the specimen has no side grooves, where B is the specimen gross thickness), and b denotes the uncracked ligament ($b = W - a$, where W is the specimen width and a is the crack length). In the above Eqn 2, plane-strain conditions are adopted such that $E' = E/(1-\nu)^2$, where E and ν are the (longitudinal) elastic modulus and Poisson's ratio, respectively. The factor η_J in Eqns 3 and 4 represents a non-dimensional parameter which relates the plastic-deformation contribution to the strain energy for the cracked body and J . Figure 1a illustrates the essential features of the estimation procedure for the plastic component J_p , where A_p (and consequently η_J) is defined in terms of load-LLD (or Δ) data or load-CMOD (or V) data. These geometry factors are denoted η_{JLLD} and η_{JCMOD} , respectively, when LLD or CMOD are used.

The incremental expression for J_p defined by Eqn 3 coupled with Eqn 4 contains two contributions: one is from the plastic work in terms of CMOD and, hence η_{JCMOD} , and the other due to crack growth correction in terms of LLD by means of η_{JLLD} ; evaluation of Eqns 3 and 4 is relatively straightforward provided that these two geometric factors are known. For the clamped SE(T) specimens with $H/W = 10$ and the conventional SE(B) specimen with $S/W = 4$ utilized in this study,

$$J_p^k = \left[J_p^{k-1} + \frac{\eta_{J-CMOD}^{k-1}}{b_{k-1}B_N} (A_p^k - A_p^{k-1}) \right] \left[1 - \frac{\gamma_{LLD}^{k-1}}{b_{k-1}} (a_k - a_{k-1}) \right] \quad (3)$$

a convenient polynomial fitting of the results given by Cravero and Ruggieri [14], Donato and Ruggieri [17], and Ruggieri [18] provides the corresponding η -factor equations for homogeneous materials in the form shown in Eqns 5-8 below.

Equations 7 and 8 applicable to SE(B) specimens agree very well with the η -factors in the revised J -integral expressions developed by Zhu *et al.* [19] which form the basis of current ASTM E1820 [6] and ISO 15653 [12] standards using CMOD records.

Crack-length estimation

Current testing protocols to measure the crack-growth-resistance response using a single-specimen test are primarily based on the unloading compliance (UC) technique to obtain accurate estimates of the current crack length from the specimen compliance measured at periodic unloadings with increased deformation. Figure 1b illustrates the essential features of the method. The slope of the load-displacement curve during the k -th unloading defines the current specimen compliance, denoted C_k , which depends on specimen geometry and crack length. For the clamped SE(T) and SE(B) specimens with $H/W = 10$ and the SE(B) specimen with $S/W = 4$ analysed here, the specimen compliance is often defined in terms of normalized quantities expressed as [6, 14]:

$$\mu_{CMOD}^{SET} = \left[1 + \sqrt{EB_e C_{CMOD}} \right]^{-1} \quad (9)$$

and

$$\mu_{CMOD}^{SEB} = \left[1 + \sqrt{\frac{EWB_e C_{CMOD}}{S/4}} \right]^{-1} \quad (10)$$

where μ_{CMOD}^{SET} and μ_{CMOD}^{SEB} define the normalized compliances for the SE(T) and SE(B) specimens. In the above expressions, E is the longitudinal elastic modulus,

C_{CMOD} denotes the specimen compliance in terms of CMOD ($C_{CMOD} = V/P$) and the effective thickness, B_e , is defined by:

$$B_e = B - \frac{(B - B_N)^2}{B} \quad (11)$$

By measuring the instantaneous compliance during unloading of the specimen (see Fig.1b), the current crack length follows directly from solving the functional dependence of crack length and specimen compliance in terms of μ_{CMOD} . For the clamped SE(T) and SE(B) specimens analysed here, the corresponding compliance expressions are given by Cravero and Ruggieri [14] and Appendix X.2 of ASTM E1820 [6] respectively as:

$$\left[\frac{a}{W} \right]_{SET} = 1.921 - 13.219\mu + 58.708\mu^2 - 155.282\mu^3 + 207.399\mu^4 - 107.917\mu^5 \quad (12)$$

$$0.1 \leq a/W \leq 0.7$$

$$\left[\frac{a}{W} \right]_{SEB} = 1.019 - 4.537\mu + 9.01\mu^2 - 27.333\mu^3 + 74.4\mu^4 - 71.489\mu^5 \quad (13)$$

$$0.05 \leq a/W \leq 0.45$$

Effect of weld strength overmatch on plastic η -factors

Current test standards employ J -estimation expressions which are mainly applicable to fracture specimens made of homogeneous materials. For a given specimen geometry, mismatch between the weld metal and base-plate strength affects the macroscopic mechanical behaviour of the specimen in terms of its load-displacement response, with a potentially strong impact on the coupling relationship between J and the near-tip stress fields.

$$\eta_{J-CMOD}^{SET} = 1.07 - 1.77 \frac{a}{W} + 7.81 \left(\frac{a}{W} \right)^2 - 18.27 \left(\frac{a}{W} \right)^3 + 15.30 \left(\frac{a}{W} \right)^4 - 3.08 \left(\frac{a}{W} \right)^5 \quad (5)$$

$$0.2 \leq a/W \leq 0.7$$

$$\eta_{J-LLD}^{SET} = -0.62 + 9.34 \frac{a}{W} - 4.58 \left(\frac{a}{W} \right)^2 - 47.96 \left(\frac{a}{W} \right)^3 + 87.70 \left(\frac{a}{W} \right)^4 - 44.88 \left(\frac{a}{W} \right)^5 \quad (6)$$

$$0.2 \leq a/W \leq 0.7$$

$$\eta_{J-CMOD}^{SEB} = 3.65 - 2.11 \frac{a}{W} + 0.34 \left(\frac{a}{W} \right)^2 \quad (7)$$

$$0.1 \leq a/W \leq 0.7$$

$$\eta_{J-LLD}^{SEB} = 0.02 + 18.09 \frac{a}{W} - 73.26 \left(\frac{a}{W} \right)^2 + 152.22 \left(\frac{a}{W} \right)^3 - 159.77 \left(\frac{a}{W} \right)^4 + 66.88 \left(\frac{a}{W} \right)^5 \quad (8)$$

$$0.1 \leq a/W \leq 0.7$$

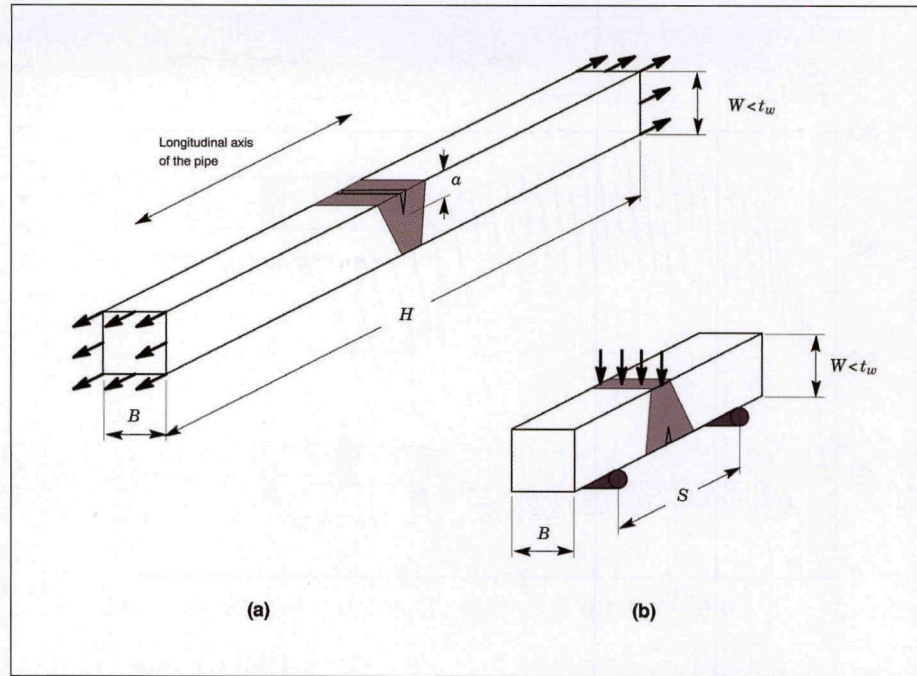


Fig.2. Geometry of tested fracture specimens with weld-centreline notch and $B \times B$ cross section:
(a) clamped SE(T) specimen with $a/W = 0.4$ and $H/W = 10$; **(b)** three-point SE(B) specimen with $a/W = 0.25$ and $S/W = 4$.

Accurate estimation formulas for J more applicable to welded fracture specimens may become important in robust defect-assessment procedures capable of including effects of weld-strength mismatch on fracture toughness.

Previous work by Donato *et al.* [20], and Paredes and Ruggieri [21], introduced a functional dependence of geometry factor η_{J-CMOD} on crack size and weld-strength mismatch for weld centreline fracture specimens. The expressions of factor η_{J-CMOD} for the weld cracked SE(B) with $S/W = 4$ and SE(T) with $H/W = 10$ are summarized as follows:

$$\begin{aligned} \eta_{J-CMOD}^{SEB} &= 3.88 + 0.22 \frac{a}{W} - 5.01 \left(\frac{a}{W} \right)^2 \\ &+ 4.02 \left(\frac{a}{W} \right)^3 - 0.41 M_y - 0.05 M_y^2 \end{aligned} \quad (14)$$

$0.2 \leq a/W \leq 0.7, 1.0 \leq M_y \leq 1.5$

$$\begin{aligned} \eta_{J-CMOD}^{SET} &= -0.36 + 11.69 \frac{a}{W} - 23.59 \left(\frac{a}{W} \right)^2 \\ &+ 13.90 \left(\frac{a}{W} \right)^3 - 0.28 M_y - 0.03 M_y^2 \end{aligned} \quad (15)$$

$0.2 \leq a/W \leq 0.7, 1.0 \leq M_y \leq 1.5$

In the above expressions, the mismatch ratio, M_y , is defined as:

$$M_y = \frac{\sigma_{ys}^{WM}}{\sigma_{ys}^{MB}} \quad (16)$$

where σ_{ys}^{MB} and σ_{ys}^{WM} denote the yield stresses for the base-plate metal and the weld metal.

Experimental details

Material description and welding procedures

The material used in this study was a high-strength, low-alloy (HSLA), API grade X-80 pipeline steel produced as a base plate using a control-rolled processing route without accelerated cooling. The mechanical properties and strength/toughness combination for this material are mainly obtained by both grain-size refinement and second-phase strengthening due to the small-size precipitates in the matrix. A 20-in diameter pipe with longitudinal seam weld from which the girth weld SE(T) and SE(B) specimens were extracted was fabricated using the UOE process.

The tested weld joint was made from the API X-80 UOE pipe having wall thickness $t_w = 19$ mm. Girth welding of the pipe was performed using the FCAW process in the 1G (flat) position with a single V-groove configuration in which the root pass was made by GMAW welding. The main weld parameters used for preparation of the test weld using the FCAW process are:

- (i) number of passes = 12 (including the root pass made by the GMAW process);
- (ii) welding current = 165 A;
- (iii) welding voltage = 23 V;
- (iv) average heat input = 1.5 kJ/mm.

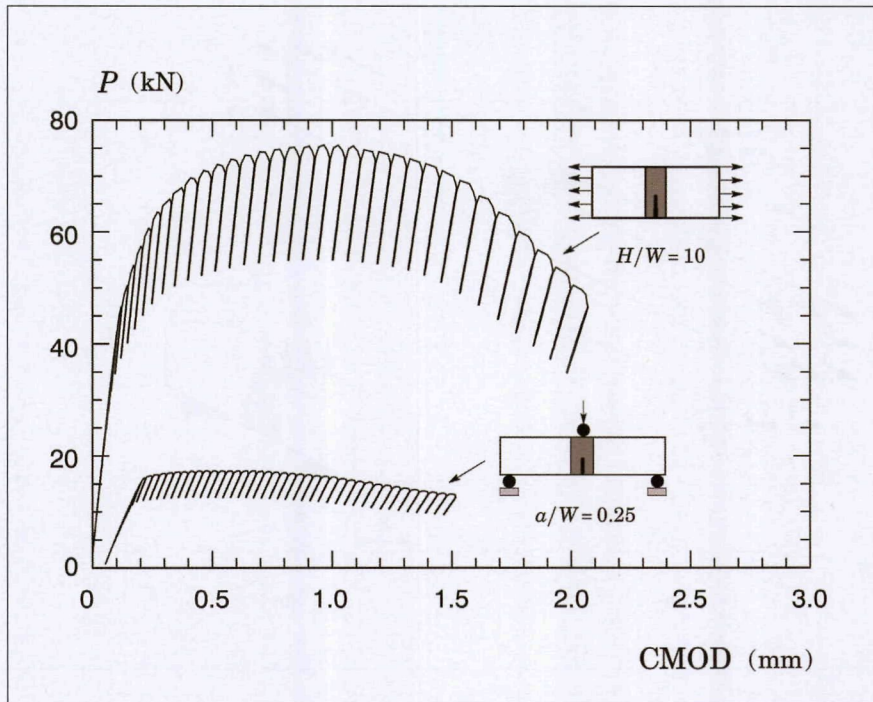


Fig.3. Measured load-CMOD curve for the tested X-80 pipeline girth weld using clamped SE(T) specimens with $a/W = 0.4$ and three-point SE(B) specimen with $a/W = 0.25$.

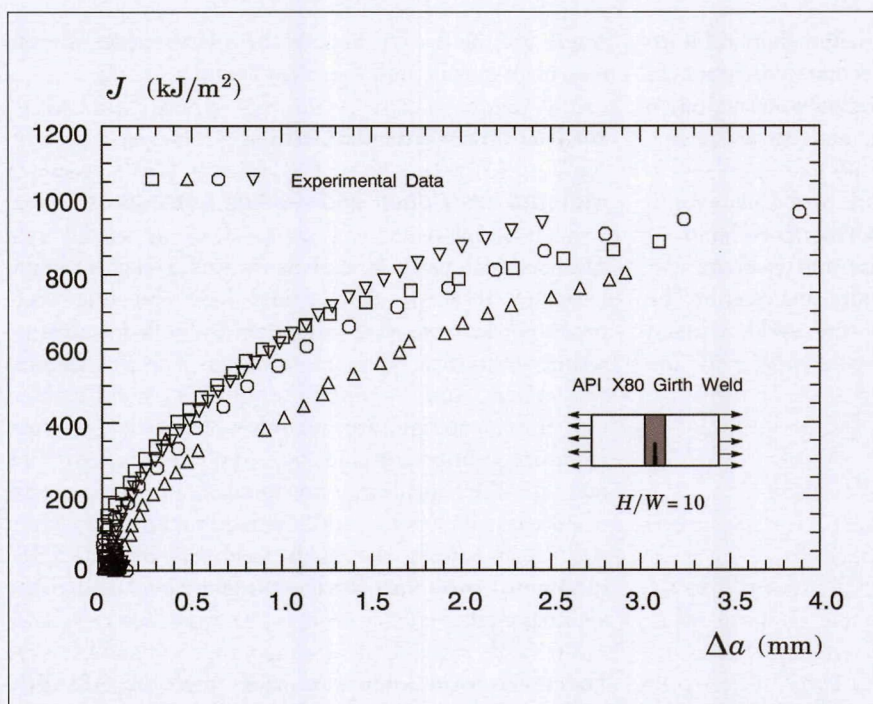


Fig.4. J -resistance curves for the clamped SE(T) specimens with $a/W = 0.4$ and $H/W = 10$.

Mathias *et al.* [22] provide the tensile properties for the tested pipeline girth weld and base material which include:

$$\begin{aligned}\sigma_{ys}^{WM} &= 715 \text{ MPa} \\ \sigma_{uts}^{WM} &= 750 \text{ MPa} \\ \sigma_{ys}^{BM} &= 609 \text{ MPa} \\ \sigma_{uts}^{BM} &= 679 \text{ MPa.}\end{aligned}$$

Here, σ_{ys} and σ_{uts} represent the material's yield stress and tensile strength, and WM and BM denote the weld metal and the base plate.

Specimen geometries

Mathias [23] conducted unloading compliance tests at room temperature on weld-centreline-notched SE(T) specimens with fixed-grip loading to measure tearing resistance curves in terms of $J - \Delta a$ data. The clamped SE(T) specimens have a fixed overall geometry and crack length to width ratio defined by $a/W = 0.4$, $H/W = 10$ with thickness $B = 14.8$ mm, width $W = 14.8$ mm ($W = B$) and clamp distance $H = 148$ mm (refer to Fig.2a). Here, a is the crack depth and W is the

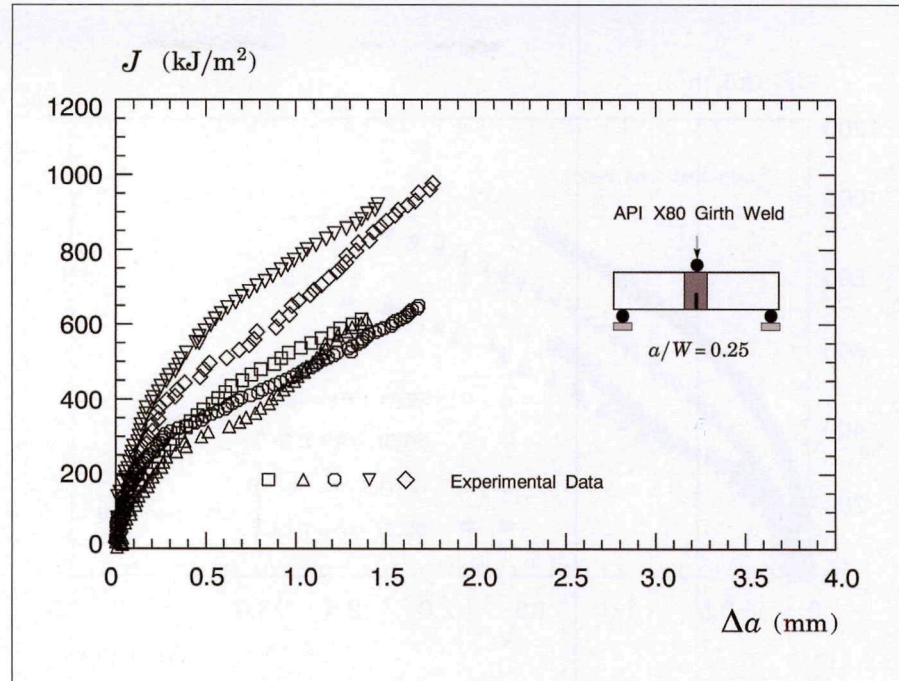


Fig.5. J -resistance curves for the three-point SE(B) specimens with $a/W = 0.25$.

specimen width which is slightly smaller than the pipe wall thickness, t_w . The UC tests at room temperature were also conducted on weld-centreline-notched SE(B) specimens with $a/W = 0.25$, specimen thickness $B = 14.8$ mm, width $W = 14.8$ mm ($B = W$) and span $S = 4W$ (refer to Fig.2b). Conducted as part of a collaborative research programme at the University of São Paulo on structural-integrity assessment of marine steel-catenary risers (SCRs), testing of these specimens focused on the development of accurate procedures to evaluate crack-growth resistance data for pipeline girth welds. Mathias *et al.* [22] provided more details on the materials used and fracture testing of the X-80 pipeline girth weld.

All specimens, including the SE(T) configuration, were pre-cracked in three-point bend conditions. After fatigue pre-cracking, the specimens were side-grooved to a net thickness of approx. 85% the overall thickness (7.5% side-groove on each side) to promote uniform crack growth along the crack front, and tested following the general guidelines described in ASTM E1820 [6]. Records of load vs CMOD were obtained for the specimens using a clip gauge mounted on knife edges attached to the specimen surface.

Crack-growth-resistance curves

Effect of specimen geometry on J -resistance curves

The framework for determining J -resistance curves based on CMOD from conventional fracture specimens described previously provides the basis for evaluating the ductile-fracture response of the tested material and assessing effects of specimen geometry and loading

mode on the $J - \Delta a$ data. We first draw attention to the load-carrying capacity for the bend and tension configurations. Figure 3 shows a typical load-CMOD curve measured from tests of the SE(T) specimen with $H/W = 10$ and $a/W = 4$, and the SE(B) specimen with $S/W = 4$ and $a/W = 0.25$. The strong effect of loading mode (tension vs bending) associated with specimen geometry is evident in this plot. At similar levels of CMOD, the applied load for the SE(T) specimen increases approximately by a factor of four compared to the load response for the SE(B) specimen.

Evaluation of the crack-growth-resistance curve follows from determining J and Δa at each unloading point of the measured load-displacement data based upon the previous formulations for the η -factors and compliance functions. Figures 4 and 5 compare the measured crack-growth-resistance curves for the SE(T) and SE(B) specimens: it can be seen that the resistance curves for the shallow-crack SE(B) specimen are comparable to the J -R curves corresponding to the deeply-cracked SE(T) specimen. Here, the average J -values at fixed amounts of crack growth, Δa , for both crack configurations are reasonably similar. Another significant features associated with these plots include:

- The average slope of the J -R curve for the SE(B) specimen (which is also related to the material's tearing modulus) is slightly higher than the corresponding slope for the SE(T) specimen.
- The estimated value of the J -integral at onset of ductile tearing, J_{lc} , is fairly independent of specimen geometry and loading mode.

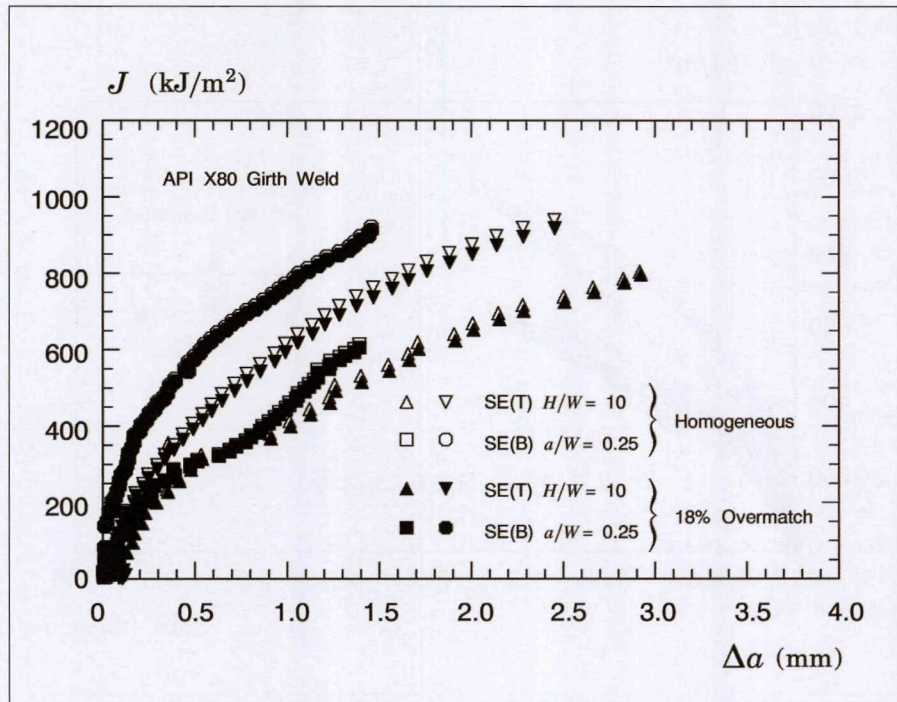


Fig.6. J -resistance curves for the SE(T) specimen and SE(B) specimen based upon η -factors for homogeneous materials and overmatched welds.

Specimen	Configuration	Measured post test			Compliance estimation		Deviation (%)
		a_0 (mm)	a_f (mm)	Δa (mm)	a_f (mm)	Δa (mm)	
SET1 H10	SE(T) H/W=10	5.66	8.79	3.13	8.77	3.11	0.78
SET2 H10	SE(T) H/W=10	6.11	8.66	2.55	8.56	2.45	3.87
SET3 H10	SE(T) H/W=10	6.29	9.32	3.03	9.20	2.92	3.75
SET4 H10	SE(T) H/W=10	6.70	10.59	3.89	10.59	3.89	0.03
SEB1	SE(B) a/W=0.25	4.38	6.28	1.90	5.89	1.39	26.84
SEB2	SE(B) a/W=0.25	4.99	7.00	2.01	6.38	1.48	26.37
SEB3	SE(B) a/W=0.25	4.48	6.65	2.17	6.12	1.78	17.97
SEB4	SE(B) a/W=0.25	3.75	6.50	2.75	5.84	1.94	29.45
SEB5	SE(B) a/W=0.25	3.93	6.25	2.32	5.30	1.65	28.88

Table 1. Predicted and measured crack extension for tested fracture specimens.

Unfortunately, the measured resistance curves are perhaps somewhat more scattered than we would expect for these specimens, particularly for the bend configuration. While we did not thoroughly investigate such behaviour, the crack-front measurements conducted by Mathias [23] revealed a somewhat highly uneven crack advance, thus providing some explanation for the scatter of the measured resistance curves. However, it is evident that the J -resistance data for the SE(B) configuration compare relatively well with the SE(T) specimen results.

Effect of weld strength overmatch on J -resistance curves

The effect of weld-strength mismatch on the fracture-resistance response characterized by the J - Δa data is examined here for the tested SE(T) and SE(B) specimens with weld-centreline notch. The primary interest is to assess the potential deviation that arises from evaluating the J -resistance curves using η equations developed for homogeneous materials.

Figure 6 compares the J -resistance curves for the shallow-crack SE(B) specimen and deep-crack SE(T) specimen based on η -factors for homogeneous materials and overmatched welds, as represented by open and solid symbols. The η -values for the overmatch condition are determined from using the estimation Eqns 14 and 15 provided previously, with $M_y = 1.18$ (refer to Eqn 16). To facilitate comparison, only the lowest and highest resistance curves for these crack configurations are included in the plot. It can be seen that the fracture-resistance curves derived from η -factors for overmatched welds are practically indistinguishable from the curves evaluated with η -factors for homogeneous materials. Here, the use of η -factors for homogeneous materials (i.e. not taking into account the degree of weld strength overmatch) leads to slightly non-conservative (higher) estimates of the resistance curve (we should emphasize that the larger the levels of weld-strength mismatch, the larger the degree of non-conservativeness).

Crack-length estimates

After testing, all specimens were subjected to heat-tinting treatment (300°C for 30 min), and then air cooled before being broken apart. Following standard methods based on the nine-point average technique, such as the procedure given by ASTM E1820 [6], the initial and final crack length measured after the test by means of an optical method were compared with crack length estimates derived from the UC method. Table 1 provides the predicted and measured crack extension for all tested fracture specimens, where the deviation is defined as:

$$\Delta a_{\text{measured}} - \Delta a_{\text{predicted}} / \Delta a_{\text{measured}}$$

The significant features that emerge from these results include:

- predictions of crack extension based on the UC procedure for the SE(T) specimens are in close agreement with experimental measurements with a level of accuracy of approx 5%;
- crack-extension predictions for the shallow-crack SE(B) configuration derived from the UC procedure are not in good agreement with the measured amount of ductile tearing; here, the UC method underestimates the nine-point average crack extension by approx. 25-30%, which produces apparent higher J -resistance curves.

The crack-growth behaviour for the shallow-crack SE(B) configuration can be explained in terms of the uneven crack advance and a rather irregular crack-front profile observed in these specimens. Figure 7 shows typical crack surfaces for the SE(B) and SE(T) configurations:

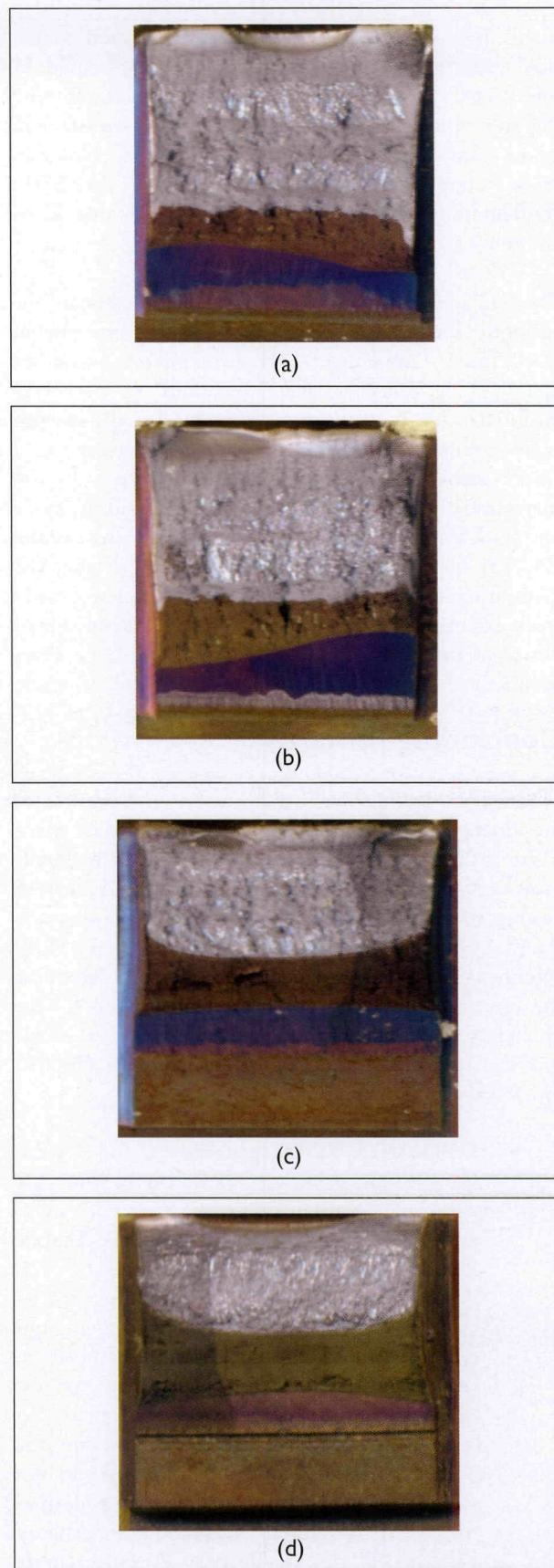


Fig. 7. Typical fracture surfaces of tested crack configurations: (a, b) three-point SE(B) specimen with $a/W = 0.25$; (c, d) clamped SE(T) specimen with $a/W = 0.4$.

it can be seen that the bend specimens exhibited a highly non-uniform fatigue pre-crack compared to the SE(T) specimens. Such a feature could be caused by unexpected misalignment between the specimen and the rollers, thereby affecting the crack-tip stresses and strains driving the ductile-fracture process. However, crack tunnelling is less pronounced for the SE(B) configuration than for the SE(T) specimen after some amount of ductile tearing.

The UC procedure described previously to estimate the current crack length involves the assumption of a straight crack front. Consequently, the compliance equations described by Eqns 12 and 13 should be viewed as idealized solutions providing estimates for the average crack extension. Moreover, the inaccurate estimate of crack extension resulting from these analyses is also suggestive of a strong effect of the bend-loading mode on crack-length predictions. Indeed, previous studies [24, 25] have already indicated that use of the UC method with three-point-bend specimens underestimates crack extension when compared with optically measured values of crack length; this effect appears to be more pronounced for SE(B) specimen with a shallow crack.

Concluding remarks

This study described an experimental investigation of the ductile-tearing properties for a girth weld made of an API 5L X-80 pipeline steel and experimentally measured crack growth resistance curves ($J - \Delta a$ curves). Testing of the pipeline girth welds used side-grooved, clamped SE(T) specimens and shallow-crack-bend SE(B) specimens with a weld-centreline notch to determine the crack-growth-resistance curves based upon the unloading compliance (UC) method using a single specimen technique. The work described here supports the following conclusions:

- Shallow-crack SE(B) specimens ($a/W = 0.25$) provide crack-growth-resistance curves which are comparable to the J -resistance curves for deep-crack SE(T) specimens ($a/W = 0.4$). Despite the relatively larger scatter of the $J - \Delta a$ data, the fracture resistance for the shallow-crack SE(B) configuration at a fixed amount of crack growth, Δa , is relatively similar to the corresponding fracture resistance for the SE(T) specimen.
- Levels of weld-strength overmatch within the range of 10-20% (approx.) overmatch do not significantly affect J -resistance curves derived from using η -values applicable to homogeneous materials. While the fracture resistance curves based on η -values for homogeneous materials are slightly higher than those based on η -factors for overmatched weldments, differences are nevertheless small and within acceptable limits.

- Crack-extension predictions based on the UC procedure agree well with experimental measurements for the SE(T) specimens. In contrast, the unloading-compliance method underestimates the nine-point average crack extension for the shallow-crack SE(B) specimen by 25-30% (approx.). This rather strong under-prediction of crack extension for this crack configuration produces apparent higher J -resistance curves and, at the same time, underlies some limitations of current UC estimation equations to predict crack length in small-sized-bend specimens.

While the analyses described here clearly provide support for using shallow-crack-bend configurations as an alternative fracture specimen to measure crack-growth properties for pipeline girth welds and similar structural components, they are also suggestive of the need for more experimental studies to validate the UC-based procedure for estimating J -resistance curves of SE(B) configurations. In particular, more-accurate techniques for crack-length estimations in small-size-bend specimens appear central to develop a robust and efficient J -resistance evaluation procedure. Additional work is in progress along these lines of investigation.

Acknowledgments

This investigation is primarily supported by Fundação de Amparo à Pesquisa do Estado de São Paulo (FAPESP) through Grant 2009/54229-3 and by Agência Nacional de Petróleo, Gás Natural e Biocombustíveis (ANP). The work of CR is also supported by the Brazilian Council for Scientific and Technological Development (CNPq) through Grants 304132/2009-8 and 476581/2009-5. The authors acknowledge Tenaris-Confab Brasil and Lincoln Electric Brasil for providing support for the experiments described in this work.

References

1. J.W.Hutchinson, 1983. Fundamentals of the phenomenological theory of nonlinear fracture mechanics.' *J. Applied Mechanics*, 50, pp 1042-1051.
2. U.Zerbst, R.A.Ainsworth, and K.-H.Schwalbe, 2000. Basic principles of analytical flaw assessment methods. *Int. J. Pressure Vessels and Piping*, 77, pp 855-867.
3. T.L.Anderson, 2005. Fracture mechanics: fundaments and applications. 3rd Edn, CRC Press, New York.
4. British Standard Institution, 2005. Guide to methods for assessing the acceptability of flaws in metallic structures, BS7910.
5. American Petroleum Institute, 2007. API Standard 579-1/ASME FFS-1, Fitness-for-service, 2nd Edn.
6. ASTM, 2011. ASTM E1820: Standard test method for measurement of fracture toughness

7. G.H.B.Donato and C.Ruggieri, 2008. Constraint effects and crack driving forces in surface cracked pipes subjected to reeling. Proc. ASME International Conference on Offshore Mechanics and Arctic Engineering (OMAE 2008), American Society of Mechanical Engineers, Lisbon, Portugal.
8. B.Nyhus, M.Polanco, and O.Orjasæter, 2003. SENT specimens as an alternative to SENB specimens for fracture mechanics testing of pipelines. Proc. ASME International Conference on Offshore Mechanics and Arctic Engineering (OMAE 2003), American Society of Mechanical Engineers, Cancun, Mexico.
9. S.Cravero and C.Ruggieri, 2005. Correlation of fracture behavior in high pressure pipelines with axial flaws using constraint designed test specimens - Part I: Plane-strain analyses. *Eng Fract. Mech.*, **72**, pp 1344-1360.
10. L.A.L.Silva, S.Cravero, and C.Ruggieri, 2006. Correlation of fracture behavior in high pressure pipelines with axial flaws using constraint designed test specimens - Part II: 3-D effects on constraint. *Idem*, **73**, pp 2123-2138.
11. D.Y.Park, W.R.Tyson, J.A.Gianetto, G.Shen, and R.S.Eagleso, 2010. Evaluation of fracture toughness of X100 pipe steel using SE(B) and clamped SE(T) single specimens. Proc. International Pipeline Conference, Calgary, Canada.
12. International Organization for Standardization, 2010. Metallic materials – method of test for the determination of quasistatic fracture toughness of welds, ISO 15653.
13. J.D.G.Sumpter and C.E.Turner, 1976. Method for laboratory determination of J_c . Cracks and Fracture, ASTM STP601, American Society for Testing and Materials, pp 3-18.
14. S.Cravero and C.Ruggieri, 2007. Estimation procedure of J -resistance curves for SE(T) fracture specimens using unloading compliance. *Eng Fract. Mech.*, **74**, pp 2735-2757.
15. Ibid., 2007. Further developments in J evaluation procedure for growing cracks based on LLD and CMOD data. *Int J. Fracture*, **148**, pp 387-400.
16. X.-K.Zhu and J.A.Joyce, 2012. Review of fracture toughness (G, K, J, CTOD, CTOA) testing and standardization. *Eng Fract. Mech.*, **85**, pp 1-46.
17. G.H.B.Donato and C.Ruggieri, 2006. Estimation procedure for J and CTOD fracture parameters using three point bend specimens. Proc. International Pipeline Conference (IPC 2006), American Society of Mechanical Engineers, Calgary, Canada.
18. C.Ruggieri, 2012. Further results in J and CTOD estimation procedures for SE(T) fracture specimens - Part I: homogeneous materials. *Eng Fract. Mech.*, **79**, pp 245-265.
19. X.-K.Zhu, B.N.Leis, and J.A.Joyce, 2008. Experimental estimation of J -R curves from load-CMOD record for SE(B) Specimens. *J. ASTM International*, **5**, JAI 101532.
20. G.H.B.Donato, R.Magnabosco, and C.Ruggieri, 2009. Effects of weld strength mismatch on J and CTOD estimation procedure for SE(B) specimens. *Int. J. Fracture*, **159**, pp 1-20.
21. M.Paredes and C.Ruggieri, 2012. Further results in J and CTOD estimation procedures for SE(T) fracture specimens - Part II: center cracked welds. *Eng Fract. Mech.*, **89**, pp 24-39.
22. L.L.S.Mathias, D.F.B.Sarzosa, and C.Ruggieri. Effects of specimen geometry and loading mode on crack growth resistance curves of a high-strength pipeline girth weld. *Int. J. Pressure Vessels and Piping* (submitted for publication).
23. L.L.S.Mathias, 2013. Experimental evaluation of J -R curves in X80 pipeline girth welds using SE(T) and SE(B) fracture specimens. Master's Thesis, Polytechnic School, University of São Paulo (*in Portuguese*).
24. P.A.J.M.Steekamp, 1988. J -R curve testing of three-point bend specimen by the unloading compliance method. Fracture Mechanics: 18th Symposium, ASTM STP 945, American Society for Testing and Materials, Philadelphia, pp 583-610.
25. J.Dzugan, 2003. Crack length calculation by the unloading compliance technique for Charpy size specimens. *Wissenschaftlich-Technische Berichte FZR-385*, Forschungszentrum Rossendorf (FZR).

Copyright of Journal of Pipeline Engineering is the property of Scientific Surveys Ltd and its content may not be copied or emailed to multiple sites or posted to a listserv without the copyright holder's express written permission. However, users may print, download, or email articles for individual use.